Structural characteristics of iridium dual-emitter organometallic compound

Silviu Polosan,[a] Iulia Corina Ciobotaru, Ionut Enculescu, and Constantin Claudiu Ciobotaru
National Institute for Materials Physics, Bucharest-Magurele 077125, Romania

(Received 10 July 2014; accepted 20 October 2014)

By combining two types of ligands, phenylpyridine and quinoline, a new type of organometallic $IrQ(ppy)_2$ compound has been synthesized, which exhibits two phosphorescences: green and red. Using an appropriate catalyst, the final $IrQ(ppy)_2$ compound has a good chemical yield up to 60% and becomes a stable dual emitter at room temperature. This compound is important because it exhibits stable red emission which is limited by the quantum yield due to the low energy band gap. As a result, an overlap between the ground state and the excited state occurs due to the vibrations that increase the nonradiative transitions, destroying the red emissions. Structural characteristics of the $IrQ(ppy)_2$ powder reveal a triclinic structure confirmed by x-ray diffraction and scanning electron microscopy images. Thermal analysis of the final compound confirms a good stability against decomposition and structural changes up to 350 °C. X-ray photoelectron spectroscopy reveals Ir–O chemical bonds and several differences between the intermediate and final compounds, such as Ir–Cl bonds. Cathodoluminescence patterns show a phosphorescent triclinic structure with a higher efficiency for the red color. Backscattering electron images prove that there is a uniform distribution of iridium ions in the $IrQ(ppy)_2$ nanocrystals.

I. INTRODUCTION

Organometallic compounds are currently the main components of organic light-emitting diodes (OLEDs),[1] but some biological applications have also been found for these substances. For example, screening technique based on the oxidation processes of some ligands, followed by the quenching of the phosphorescence in the presence of cellular oxygen, seems to be a promising biological application.[2,3]

Iridium complex compounds have attracted attention as emitters for efficient electrophosphorescent devices. Special attention has been devoted for the compounds with different types of ligands and several attempts have been made to find proper ligands that generate white light.[4] The most effective approach is to find an organometallic compound with three types of ligands that can emit three colors based on its phosphorescent properties. Another way to produce such a mixture of colors is to extend the structure of the ligands by adding heavy ions or radicals, which changes the electronic distribution of the ligands.[5,6]

Until now, there have been few examples of iridium cyclometalated molecules that exhibit red emission in full color RGB displays,[7] because the low energy band gap of the red emission (or phosphorescence) generally limits its quantum yield.[8] As a result, an overlap between the ground state and the excited state occurs due to the vibrations that increase the nonradiative transitions, destroying the red emissions.

As a consequence, finding new complexes that provide red emissions is a continuous challenge. Red emission compounds can be synthesized using heteroleptic complexes, such as 2-phenylquinoxaline,[9] or with a 2-pyrazinecarboxylic acid substituent. In the case of 2-phenylquinoxaline, a lower band gap occurs because of the delocalization of the *p* electrons from the aromatic ligand chromophore, which is dominated by the Ir–N bonds and complex combinations of Ir–O bonds from the ancillary ligands. From this point of view, $IrQ(ppy)_2$ seems to be a stable red emitter compound.

The most important parameters of the organometallic compounds which can be used in the OLED technology are high decomposition and glass transition temperatures. For example, a decomposition temperature over 300 °C should be high enough to deposit molecules without any decomposition under reduced pressure.[10] Secondly, a glass transition temperature over 110 °C should be enough to exceed the joule effects which occur during the operation of the OLED devices.[11]

$IrQ(ppy)_2$ combines two types of ligands, phenylpyridine for green phosphorescence and quinoline for red phosphorescence. Organometallic complexes like $IrQ(ppy)_2$–5Cl or $IrQ(ppy)_2$–$5CH_3$ have triclinic or monoclinic structure, but have weak red emission compared with their green emission.[12] This study presents the synthesis and structural characterization of $IrQ(ppy)_2$

[a]Address all correspondence to this author.
e-mail: silv@infim.ro
DOI: 10.1557/jmr.2014.337

 © Materials Research Society 2014

https://doi.org/10.1557/jmr.2014.337 Published online by Cambridge University Press

organometallic compound. Several methods were used to identify their crystallographic structure, such as x-ray diffraction (XRD) and scanning electron microscopy (SEM), together with specific measurements concerning the thermal behavior of $IrQ(ppy)_2$ organometallic compound, namely, thermogravimetric analysis (TGA) and differential scanning calorimetry (DSC). Moreover, to determine the nature of bonds around iridium ions, the x-ray photoelectron spectroscopy (XPS) and backscattering electrons (BSE) were used. To study the emissive properties of the $IrQ(ppy)_2$ under an electron beam, the cathodoluminescence (CL) spectrum and the image patterns for the red monochromated light were examined. The purity of the final compound was checked with nuclear magnetic resonance (NMR).

II. EXPERIMENTAL

A. Synthesis

To synthesize the $IrQ(ppy)_2$ compound, a two-step reaction procedure was used.[13] In the first step, iridium chloride reacts with phenylpyridine, forming a $[(C\hat{}N)_2Ir\text{-}\mu\text{-}Cl]_2$ bridged dimer, which will be referred to as the "intermediate compound" hereinafter. A mixture of 2-phenylpyridine (ppy), 2-ethoxyethanol, and iridium chloride hexahydrate was heated to reflux under a nitrogen atmosphere for 24 h. The yellow precipitate was cooled and washed with ethanol and then dried in vacuum. The chemical yield varied between 75 and 80%. The second step involved the reaction of the intermediate compound with 8-hydroxyquinoline leading to the formation of the final complex, $IrQ(ppy)_2$ in which the mixture of 2-ethoxyethanol, $[(C\hat{}N)_2Ir\text{-}\mu\text{-}Cl]_2$, 8-hydroxyquinoline, and sodium carbonate was heated to reflux under a nitrogen atmosphere for 24 h (Fig. 1).

It was then cooled to room temperature and filtered to extract the precipitate from 2-ethoxyethanol. The crude product was dissolved in dichloromethane and filtered to remove the sodium carbonate catalysts. The $IrQ(ppy)_2$ powder was obtained after crystallization from dichloromethane and dried 12 h at 60 °C. The chemical yield for the final compound varied between 55 and 60%.

B. Characterization

The XRD measurements were performed on a BRUKER D8 ADVANCE type x-ray diffractometer (Karlsruhe, Germany), in focusing geometry, equipped with copper target x-ray tube and LynxEye one-dimensional detector, using $CuK_{\alpha 1}$ radiation ($\lambda = 1.54056$ Å), at 40 kV and 40 mA. The 2θ scan range was 5–20°, with a step size of 0.02° and a resolution of 0.01°. The line width was determined after subtraction of $K_{\alpha 2}$ lines from the $K_{\alpha 1}$–$K_{\alpha 2}$ doublet, using the Rachinger algorithm with the Bruker Difrac^{plus} Basic Evaluation program package.[14] The entire spectrum was refined by using Crystal Sleuth software[15] to determine the crystallographic behavior of the final compound.

A Zeiss EVO 50 SEM (Berlin, Germany) with a LaB_6 cathode with the Bruker EDX system was also used. Based on the SEM images, the equipment may generate secondary electrons (SEs), backscattered electrons, characteristic x-ray and CL. All SEM and CL images are taken under 30 kV electron beams. TGA of the samples was conducted on Q500 TA equipment, using nitrogen atmosphere from 20 to 800 °C with 10 °C/min heating rate. For the DSC, NETZSCH DSC 204 F1 equipment (Selb, Germany) with an aluminum crucible was used. The temperature range was set between 20 and 400 °C, with a 10 °C/min heating rate in nitrogen atmosphere. The XPS spectra were recorded on Thermo Scientific K-Alpha equipment, fully integrated, with an aluminum anode monochromatic source. Survey scans (0–1200 eV) were performed to identify the composition of the intermediate and final compounds.

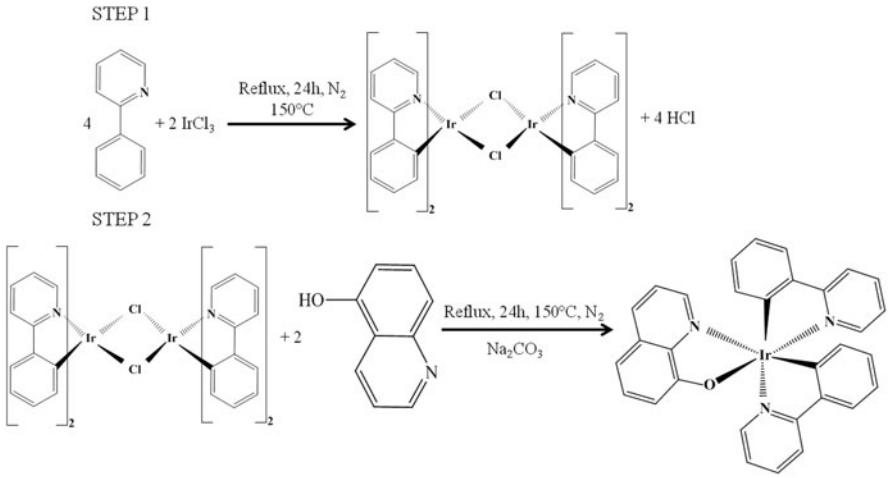


FIG. 1. Two-step synthesis of the $IrQ(ppy)_2$ compound.

https://doi.org/10.1557/jmr.2014.337 Published online by Cambridge University Press

NMR measurements were performed in chloroform, which was used as a NMR standard solvent. NMR was performed with a Bruker Advance DRX 400 MHz (BioSpin, Rheinstetten, Germany) at room temperature (approximately 26 °C).

III. RESULTS AND DISCUSSION

The ^{1}H NMR spectrum is dominated by chemical shifts from the phenylpyridine ligand, with a few shifts from quinoline: 7.99 ppm (1H, d), 7.66 ppm (1H, q), and 7.05 ppm (1H, d) for the pyridine ring; 6.79 ppm (4H, m) and 6.27 ppm (1H, d) for the phenolic ring. These shifts are in good agreement with those of the similar compound, IrQ(ppy)$_2$–5Cl.

Organometallic compounds with two different types of ligands, in which Cl and CH_3 replace the hydrogen ions in the quinoline ring, show similar structures, i.e., monoclinic and triclinic, respectively.[12] The secondary phase appears to be due to a reduced chemical yield, which, in our case, varies between 55 and 60%. It is important to mention that, without the recrystallization process following the filtration procedure of the final compound, a rather amorphous structure was observed, which was probably influenced by other compounds added as catalysts.

Figure 2 shows the XRD patterns of IrQ(ppy)$_2$ after crystallization from dichloromethane. The main peaks are assigned to a triclinic structure but some peaks suggest a secondary phase that appears during the chemical reaction. Data collection and refinement parameters for this triclinic structure, with *P-1* symmetry, have the following parameters $a = 10.3$; $b = 13.0$; $c = 13.8$; $\alpha = 65.6°$; $\beta = 86.7°$; $\gamma = 60°$ and a volume structure of $V = 1500$.

To investigate the thermal stability of the organometallic compounds, TGA and DSC were performed.

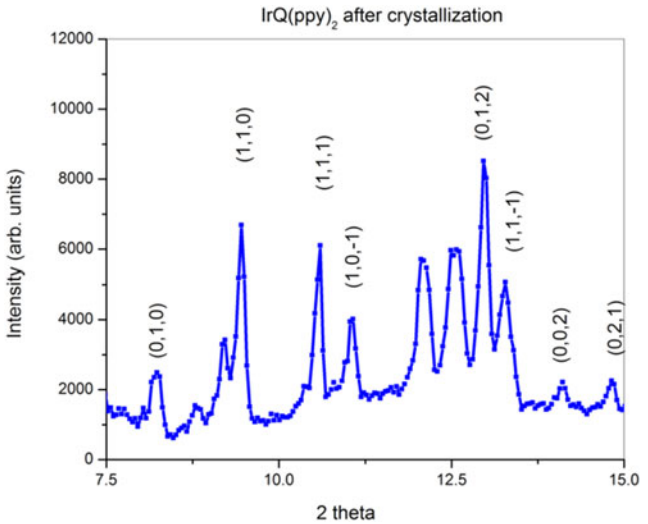


FIG. 2. XRD patterns of IrQ(ppy)$_2$ after recrystallization.

TGA of the intermediate and the final compounds is shown in Figs. 3(a) and 3(b). For the intermediate compound, the TGA curve shows a small mass decreasing by 3.3% with a sharp peak at around 205 °C in the derivative signal, followed by a strong decrease of about 15% with a peak centered at 465 °C.

Following the molecular masses involved in the intermediate compound (1076.24 g/mol), these peaks can be assigned to the broken dimer that releases the chlorine ions in the first step and the phenylpyridine ring (155.22 g/mol) in the second step. This fact is supported by the similar behavior of the well-known Ir(ppy)$_3$ compound, which exhibits a weight loss greater than 5% at approximately 423 °C.[16]

In the case of some mixed ligands, the weight loss is different, depending on the type of ligand in question. For example, the mer-Ir(dfpypy)$_3$ compound exhibits over 5% weight loss centered at 384 °C compared with the fac-Ir(dfpypy)$_3$ which has weight loss centered at 452 °C.[10] In our case, the weight loss is centered at approximately 365 °C, the temperature decrease being due to the weak coupling of the quinoline ligands with the compound resulting from the chemical reaction with the intermediate compound.[5] In fact, the relatively low decomposition temperature is related to the weak hybridization between the iridium and quinoline ligands through Ir–O bond.

Concerning the DSC curve shown in Fig. 4, the intermediate compound exhibits a relatively low stability, with an endothermic peak at around 206 °C, which begins at about 177 °C and ends at 227 °C, with an enthalpy of approximately 13.12 J/g. In the case of the final compound, DSC patterns show a higher stability, the melting point being centered at around 355 and 390 °C with an enthalpy of about 28.64 J/g. These peaks are assigned to the melting process of the mixed IrQ(ppy)$_2$ compound.

In DSC patterns, a small decreasing step at approximately 157 °C is observed, and can be assigned to the glass transition temperature, T_g. This fact is similar to the case of mer-Ir(dfpypy)$_3$, for which T_g was observed at 159.8 °C with a melting point at 383 °C, according to DSC experiments.[10] Even if the endothermic peak at 206 °C is somehow asymmetric, the coincidence between DSC and the derivative weight in the TGA at 205 °C leads to a structural change of the intermediate compound which releases the chlorine ions.

To investigate the elemental composition of the intermediate and final compounds, the XPS technique was used, particularly to point out the changes in the 4f states of the Ir ions. The core level spectra were registered using a hemispherical energy analyzer for electron detection with an energy resolution of 100 meV. A complete survey of the XPS spectra for the intermediate and the final compounds reveals some

https://doi.org/10.1557/jmr.2014.337 Published online by Cambridge University Press

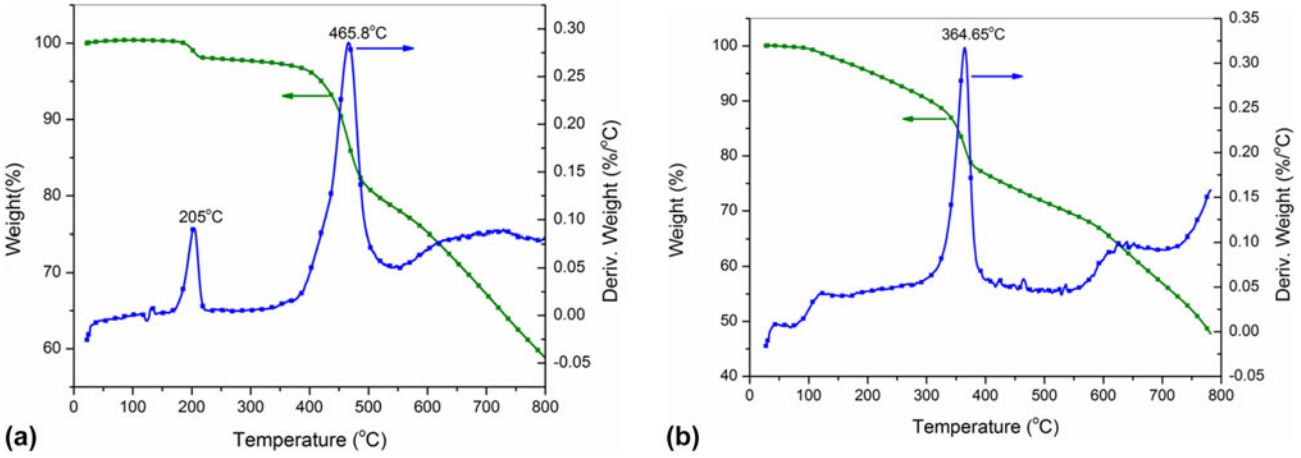


FIG. 3. (a) TGA of the intermediate compound. (b) TGA of the final compound.

interesting features, some of which are theoretically predicted (Fig. 5). The intermediate compound shows a large concentration of the chlorine 2*p* photoemission at 198.3 eV, which is almost completely absent in the final compound. Moreover, the oxygen 1*s* photoemission of the final compound at 531.4 eV is enhanced compared with intermediate compound. The photoemission peak of Na 1*s* at 1072 eV comes from Na_2CO_3 which was added as a catalyst and which increases the rate of the chemical reaction by reducing the activation energy. This remains unchanged during the reaction. Traces of Na do not affect the spectroscopic characteristics of the final compound.

The $4f_{7/2}$ seems to have the same position in both compounds, at 61.4 ± 0.1 eV, while the $4f_{5/2}$ is situated at 64.1 ± 0.1 eV [Figs. 6(a) and 6(b)]. The binding energy of the Ir $4f_{7/2}$ core level for metallic Ir is centered at 60.8 eV and the splitting of the $4f_{7/2}$–$4f_{5/2}$ doublet is 2.9 eV.[17] The ratio between $4f_{7/2}$–$4f_{5/2}$ intensities was maintained at 4:3 in all the fitting procedures.

The main difference in the XPS spectra between the intermediate and the final compound is related to the presence of 64.8 ± 0.1 and 66.3 ± 0.1 eV peaks in the intermediate compound in the dimer configuration. The first peak at 64.8 ± 0.1 eV is attributed to the Ir–Cl by comparison with other similar compounds.[18] The presence of the peak from 66.3 ± 0.1 is controversial. The appearance of this peak is apparently without chemical backup and it has been explained as being a result of the final state screening responses, i.e., conduction band interaction during the photoemission process.[19] This peak does not appear in the spectrum of the final compound. For the final compound, the presence of the peak centered at 63.06 ± 0.1 eV could be assigned to Ir–O bond from the quinoline ligand, by comparison with IrO_x compounds.[20]

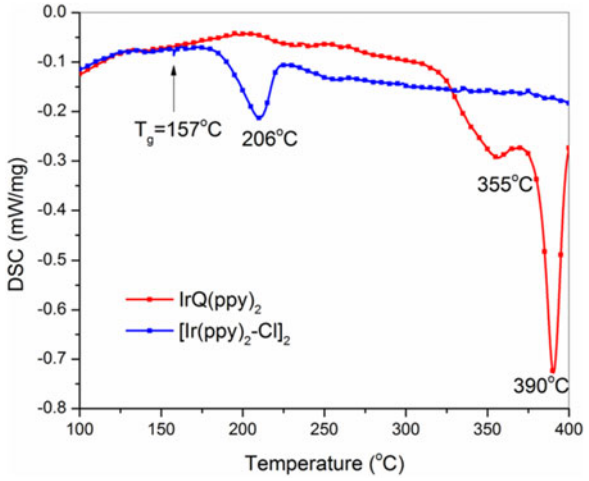


FIG. 4. DSC patterns of the intermediate and final compound.

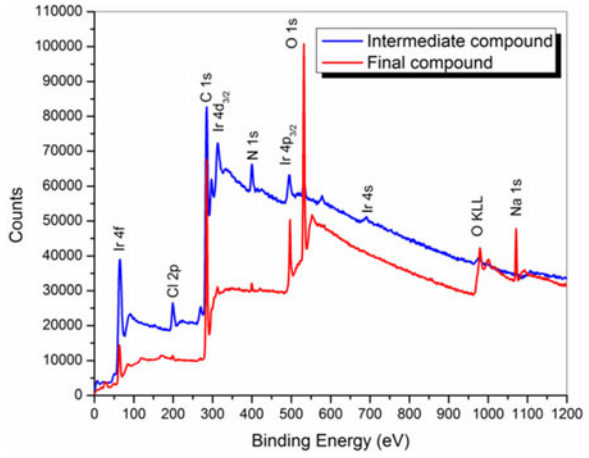


FIG. 5. XPS survey scans of the intermediate and final compound.

https://doi.org/10.1557/jmr.2014.337 Published online by Cambridge University Press

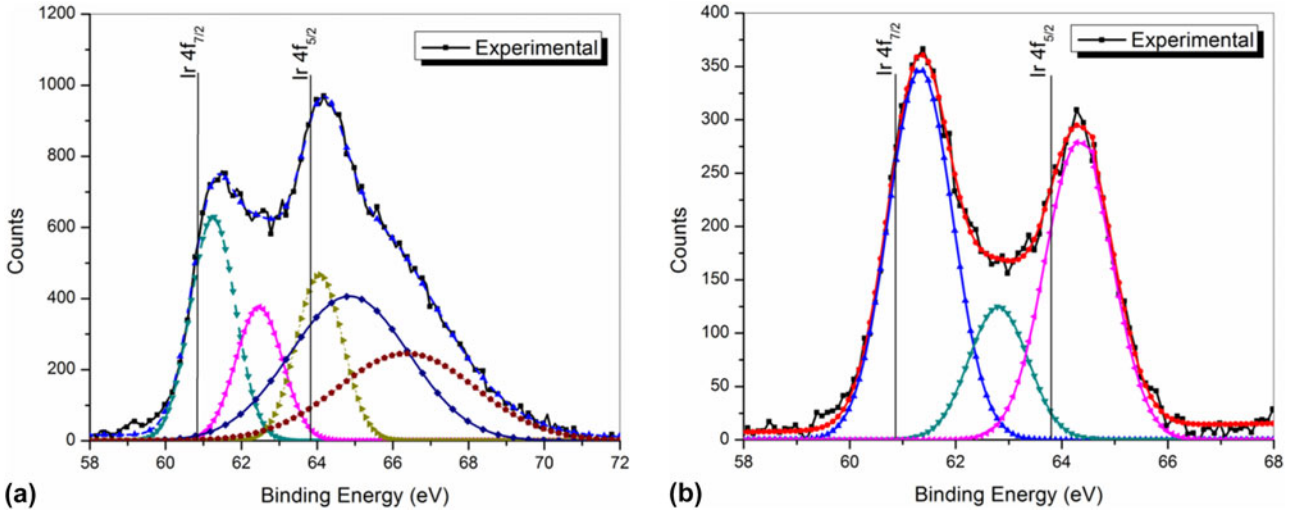


FIG. 6. (a) Ir 4f XPS spectrum of the intermediate compound. (b) Ir 4f XPS spectrum of the $IrQ(ppy)_2$.

The CL technique is closely related to the photoluminescence (PL) spectroscopy due to their incoherent part of the emission. Basically, the sample is excited with electrons, after which decays inelastically and emits light in the visible region. The most important difference between CL and PL is the excitation source, which in this case is an electron beam. Excitation with an external light is coupled with strong dipole modes. The electron beam can excite metastable levels,[21] because they are capable of transferring large momenta to the sample under investigation. This method is quite useful for the study of the organometallic compounds because of the primary property of these materials: emission from the triplet states, as in the case of Alq_3 which contain also quinoline ligands.[22] Under 30 kV electron beam the CL spectrum shows two main peaks, one at 530 nm (2.34 eV) and another, more intense peak at 635 nm (1.95 eV), the spectrum being measured on powder.

Figure 7 shows the CL image patterns of the $IrQ(ppy)_2$ compound in monochromatic light centered at 635 nm (1.95 eV), in which the triclinic structure of the nanocrystals can be distinguished. It can be seen that some of them are dispersed, while some are in aggregated structures.

The CL spectrum is similar to the PL spectrum of $IrQ(ppy)_2$–5Cl embedded in the polystyrene matrix, but the intensity of the red emission is greater than that of green.[6] This fact confirms the dual emitter characteristic of the $IrQ(ppy)_2$ organometallic compound.

The SEM images show the formation of some triclinic structures by recording the SE profile. In Fig. 8, a comparative image between CL and SE images reveals the same structures on a relative large spot size under an electron beam of 30 kV. The size of the luminescent structures is approximately 30 μm.

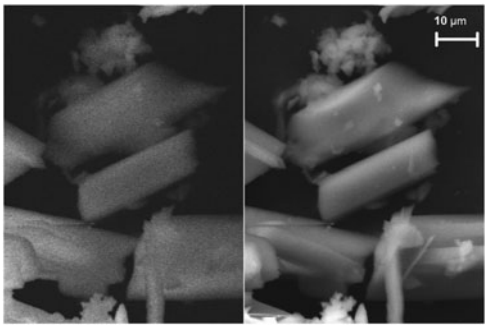


FIG. 7. Cathodoluminescence and SEM images of the final compound

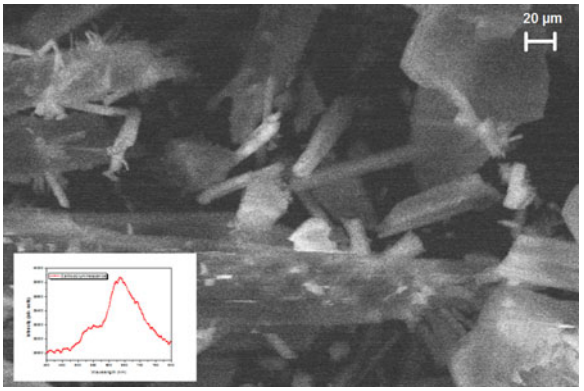


FIG. 8. Cathodoluminescence image and spectrum of the $IrQ(ppy)_2$.

To identify the spatial distribution of the iridium ions in the $IrQ(ppy)_2$ compound, a BSE image was taken (Fig. 9). Larger atoms (with a greater atomic number, Z) have a higher probability of producing an elastic collision because of their greater cross-sectional area. Consequently, the number of backscattered electrons reaching a BSE detector is proportional to the mean atomic number of the sample.

https://doi.org/10.1557/jmr.2014.337 Published online by Cambridge University Press

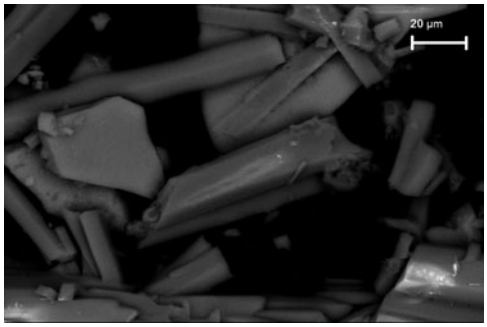


FIG. 9. Backscattering electron image of the $IrQ(ppy)_2$.

A "brighter" BSE intensity correlates with greater average *Z* in the sample, and "dark" areas have lower average *Z*. In our sample, the iridium atoms are considered to be the larger atoms, compared with the *Z* of the other elements (C, O, N, H) and the BSE images show a relatively uniform distribution of iridium ions.

IV. CONCLUSIONS

A dual emitter $IrQ(ppy)_2$ organometallic compound was synthesized by combining two types of ligands (phenylpyridine and quinoline), with green and red emissions, following a classical two-step reaction. The chemical yield varied between 55 and 60%. The purity of the final compound was checked with the NMR measurements, which confirmed that the structure contained the two types of ligands.

XRD patterns of partially crystalline powder, obtained from dichloromethane, show a *P-1* triclinic structure, which was confirmed by SEM and CL images. DSC patterns of the intermediate compound show decomposition of the bridged dimer in two steps, firstly due to the chlorine release and then by phenylpyridine decomposition. For the final compound $IrQ(ppy)_2$, a single exothermic peak was found and assigned to decomposition of the mixed ligands.

The XPS peak positions of the 4f levels of iridium show different behaviors between the intermediate and final compounds. The intermediate compound shows several peaks assigned to iridium-chloride in the bridged dimer and Ir–Cl bonds, respectively. Through comparison with IrO_x compounds, in $IrQ(ppy)_2$, the peak centered at 63.06 ± 0.1 eV could be attributed to the Ir–O bond. The SEM images show a polycrystalline structure in both samples and a relatively uniform distribution of iridium ions in the backscattering electron images.

The CL spectrum between 400 and 800 nm indicates two peaks centered at 530 nm (green emission) and 635 nm (red emission) and the CL image, in monochromatic light at 635 nm, confirms a triclinic phosphorescent organometallic compound.

ACKNOWLEDGMENT

This work was supported by a grant of the Romanian National Authority for Scientific Research, CNCS-UEFISCDI, project number PN-II-ID-PCE-2011-3-0620.

REFERENCES

1. Q. Yang, Y. Hao, Z. Wang, Y. Li, H. Wang, and B. Xu: Double-emission-layer green phosphorescent OLED based on LiF-doped TPBi as electron transport layer for improving efficiency and operational lifetime. *Synth. Met.* **162**, 398 (2012).
2. F.P. Rosselli, W.G. Quirino, C. Legnani, V.L. Calil, K.C. Teixeira, A.A. Leitão, R.B. Capaz, M. Cremona, and C.A. Achete: Experimental and theoretical investigation of tris-(8-hydroxy-quinolinate) aluminum (Alq_3) photo degradation. *Org. Electron.* **10**, 1417 (2009).
3. J. Shinar and R. Shinar: Organic light-emitting devices (OLEDs) and OLED-based chemical and biological sensors: An overview. *J. Phys. D: Appl. Phys.* **41**, 133001 (2008).
4. C.H. Mao, J.L. Hong, and A.C. Yeh: Influence of aggregation on the phosphorescence of iridium complex in poly(methyl methacrylate) matrix. *J. Polym. Sci. B* **46**, 631 (2008).
5. S. Polosan and I.C. Radu: Mechanisms of the charge transfer in $IrQ(ppy)_2$–5Cl dual-emitter compound. *J. Nanosci. Nanotechnol.* **13**, 5203 (2013).
6. S. Polosan, I.C. Radu, and T. Tsuboi: Photoluminescence and magnetic circular dichroism of $IrQ(ppy)_2$-5Cl. *J. Lumin.* **132**, 998 (2012).
7. N. Sengottuvelan, S.J. Yun, D.Y. Kim, I.H. Hwang, S.K. Kang, and Y.I. Kim: Highly efficient red emissive heteroleptic cyclometalated iridium(III) complexes bearing two substituted 2-phenylquinoxaline and one 2-pyrazinecarboxylic acid. *Bull. Korean Chem. Soc.* **34**, 167 (2013).
8. N. Bera, N. Cumpustey, P.L. Burn, and I.D.W. Samuel: Highly branched phosphorescent dendrimers for efficient solution-processed organic light-emitting diodes. *Adv. Funct. Mater.* **17**, 1149 (2007).
9. N. Sengottuvelan, H.J. Seo, S.K. Kang, and Y.I. Kim: Tuning photophysical and electrochemical properties of heteroleptic cationic iridium(III) complexes containing substituted 2-phenylquinoxaline and biimidazole. *Bull. Korean Chem. Soc.* **31**, 2309 (2010).
10. N. Jung, E. Lee, J. Kim, H. Park, K.M. Park, and Y. Kang: Synthesis and crystal structure of blue phosphorescent mer-tris (2',6'-difluoro-2,3'-bipyridinato-N,C4')iridium(III). *Bull. Korean Chem. Soc.* **33**, 183 (2012).
11. M.M. Rothmann, E. Fuchs, C. Schildknecht, N. Langer, C. Lennartz, I. Munster, and P. Strohriegl: Designing a bipolar host material for blue phosphorescent OLEDs: Phenoxy-carbazole substituted triazine. *Org. Electron.* **12**, 1192 (2011).
12. D.F. Huang, T.J. Chow, C.Y. Wu, S.S. Sun, S.H. Tsai, Y.S. Wen, S. Polosan, and T. Tsuboi: The preparation of (8-hydroxyquinolinato)bis(2-phenylpyridyl)iridium complexes and their photophysical properties. *J. Chin. Chem. Soc.* **55**, 439 (2008).
13. C. Yi, C.J. Yang, J. Liu, M. Xu, J.H. Wang, Q.Y. Cao, and X.C. Gao: Red to near-infrared electrophosphorescence from an iridium complex coordinated with 2-phenylpyridine and 8-hydroxyquinoline. *Inorg. Chim. Acta* **360**, 3493 (2007).
14. W.A. Rachinger: A correction for the α_1 α_2 doublet in the measurement of widths of x-ray diffraction lines. *J. Sci. Instrum.* **25**, 254 (1948).

https://doi.org/10.1557/jmr.2014.337 Published online by Cambridge University Press

15. T. Laetsch and R. Downs: Software for identification and refinement of cell parameters from powder diffraction data of minerals using the RRUFF project and American Mineralogist Crystal Structure Databases. Abstracts from the 19th General Meeting of the International Mineralogical Association, Kobe, Japan, 23–28 July (2006).
16. J. Lee, K.M. Park, K. Yang, and Y. Kang: Blue phosphorescent Ir(III) complex with high color purity: fac-tris(2′,6′-difluoro-2,3′-bipyridinato-N,C4′)iridium(III). *Inorg. Chem.* **48**, 1030 (2009).
17. C.D. Wagner, W.M. Riggs, L.E. Davis, and J.F. Moulder: *Handbook of X-ray Photoelectron Spectroscopy*, G.E. Muilenberg ed.; Perkin Elmer, Physical Electronics Division: Eden Prairie, MN, 1978.
18. B.D. El-Issa, A. Katrib, R. Ghodsian, B.A. Salsa, and S.H. Addassi: A comparative study of the bonding in different halides of iridium. *Int. J. Quantum Chem.* **33**, 195 (1988).
19. L. Atanasoska, R. Atanasoska, and S. Trassati: XPS and AES study of mixed layers of RuO_2 and IrO_2. *Vaccum* **40**, 91 (1990).
20. L. Atanasoska, P. Gupta, C. Deng, R. Warner, S. Larson, and J. Thompson: XPS, AES, and electrochemical study of iridium oxide coating materials for cardiovascular stent application. *ECS Trans.* **16**, 37 (2009).
21. F.J. García de Abajo: Optical excitations in electron microscopy. *Rev. Mod. Phys.* **82**, 209 (2010).
22. I.C. Radu, S. Polosan, I. Enculescu, and H. Iovu: Cathodoluminescence and Raman analysis of the finite-size effects in mer-Alq_3 structure. *Opt. Mater.* **35**, 268 (2012).

https://doi.org/10.1557/jmr.2014.337 Published online by Cambridge University Press